An Optimized M-ary Amplitude Phase Shift Keying Scheme for Ultrabroadband Terahertz Communication

Priyangshu Sen
Department of ECE
Northeastern University
Boston, MA USA
sen.pr@northeastern.edu

Viduneth Ariyarathna
Department of ECE
Northeastern University
Boston, MA USA
v.ariyarathna@northeastern.edu

Josep M. Jornet
Department of ECE
Northeastern University
Boston, MA USA
j.jornet@northeastern.edu

2022 IEEE 19th Annual Consumer Communications & Networking Conference (CCNC) | 978-1-6654-3161-3/22/$31.00 ©2022 IEEE | DOI: 10.1109/CCNC49033.2022.9700581

***Abstract*—Terahertz (THz) band (0.1 THz to 10 THz) communication is envisioned as a key technology to satisfy the demand for Terabit-per-second (Tbps) links in the sixth generation (6G) wireless systems and beyond. Significant progress within different device technologies is finally closing the so-called THz technology gap. However, there are notable limitations relating to the efficiency and reliability of THz devices. In order to overcome the challenges, innovative ways of digital signal processing, as well as waveform design techniques, need to be considered. In this context, to simultaneously overcome the limitations due to peak to average power ratio (PAPR) and reduce the effective symbol error rate (SER), both while using a high-order modulation scheme for ultrabroadband THz communication, the utilization of m-ary amplitude phase shift keying (M-APSK) is proposed. After optimizing the constellation with the number of rings as a constraint, the performance of the scheme is compared with M-ary quadrature amplitude modulation (M-QAM) and M-ary phase-shift keying (M-PSK) in terms of SER and PAPR. As a proof of concept, experimental results are provided to demonstrate the performance of the proposed scheme in the 120-140 GHz band, achieving bit-rates of up to 50 Gbps on a single-carrier, single-channel tens-of-meters-long link. This constellation will serve as a building block for multi-carrier modulations able to reach the 1 Tbps goal.**

***Index Terms*—Terahertz communications; ultrabroadband waveform and modulation design; experimental research; 6G**

I. Introduction

The already being rolled out fifth generation (5G) communication systems promise up to 20 Giga-bits-per-second (Gbps) bit-rates. IEEE 802.11ay networks, with channel bonding up to 8.6 GHz of bandwidth, promise up to about 44 Gbps rates per spatial stream. Owing to these speeds and with the non-stoppable increase in the number of mobile connected terminals, Terabit-per-second (Tbps) data-rates will have to become a reality within the next few years—especially, to aggregate the faster than ever front-haul traffic.

Scoring the Tbps data rates in wireless links will require the amalgamation of different aspects. The capacity of a wireless link depends (i) on the system bandwidth, (ii) the SNR at the receiver, and (iii) the spectral efficiency. Since the spectrum up to 100 GHz has already been allocated, the next-generation networks are relying on the terahertz (THz) band to find the bandwidth needed. Much progress has happened to closing the THz gap in terms of front-end electronics [1] besides understanding the wireless channels at these frequencies [2].

Although a huge amount of uncharted of bandwidth exists above 100 GHz frequencies, having the bandwidth itself will not pave the path for the race to achieving Tbps rates. Therefore, it is essential that maximum spectral efficiency is utilized and higher spatial multiplexing is integrated to the system. Multiple-input multiple-output spatial multiplexing techniques will continue to benefit systems above 100 GHz [3]. Before that, however, there is plenty of room for innovative approaches to waveform design to achieve higher capacity links addressing the peculiarities of the THz band.

Higher-order M-QAM schemes have been the most established modulation option to achieve high spectral efficiency. However, higher-order QAM modulations suffer from high Peak-to-Average Power Ratio (PAPR), which limits the modulation order used in practice. This becomes much significant in THz systems where strict output power limitations exist [4]. This is mainly due to the device technologies at these frequencies, where the efficiencies of the power amplifiers (PAs) and other front-end electronics are much lower [5].

Moreover, the transmitted signal experiences different types of noise, including phase noise by frequency-multiplying chains at the transceiver, molecular absorption noise by the channel, and comparatively high noise figures associated with the THz receiver chain (including mixers and amplifiers) compared to low frequency counter parts [6]. Further, the low-noise amplifier (LNA) linearity degrade with an increase in frequency [7]. Therefore, utilization of high-order M-PSK in terms of SER performance is not a valid option.

Many recent efforts can be identified for designing practical signal processing schemes targeting ultrabroadband THz communication [8]. The recent IEEE 802.15.3d standard [9] for lower THz frequency range 252–325 GHz targeting 100 Gbps wireless switched point-to-point links is one such step, which considers single-carrier schemes with low-order modulation indexes. Also, significant research work is conducted to reduce the PAPR of the multi-carrier scheme, such as discrete Fourier transform spread orthogonal frequency division multiplexing (DFT-S-OFDM) [10]. However, few notable efforts are provided

This work was supported by the U.S. National Science Foundation Grant No. CNS-2011411

to reduce the PAPR at the constellation level while maintaining low SER, which can then serve as a feed to OFDM blocks.

In this paper, we propose M-APSK scheme for reliable, low-PAPR, and spectrally-efficient ultrabroadband THz communication. The modulation design is based on arranging the constellation points in a number of concentric rings, similar to PSK. The number of points in each ring proportionally varies with its amplitude, maintaining the same minimum distance within adjacent points. Thus, there are fewer points in an inner circle compared to the outer. Concentric ring amplitude and phase modulations were introduced over fifty years ago [11], and several works have been done subsequently, suggesting differential encoding as well as error-correcting coding techniques [12]–[14] to increase the reliability of the scheme. In most cases, the study is confined to APSK utilized in digital video broadcasting for satellite applications (i.e., DVB-S2) [15], which have a specific constellation design considering the fixed number of rings. Although closed-form symbol error rate (SER) expressions have been investigated for APSK in DVB-S2 standard [16], [17], limited work has been done towards obtaining a generalized closed-form SER expression for M-APSK with a varying number of rings and modulation index (M). Further, the optimization of the constellation to minimize the SER, the study of the impact of the number of rings with a constrain on the maximum number of rings for particular M, and the advantages in terms of PAPR with decreasing number of rings have not been explored. Instead, in this paper, we optimize the constellation of M-APSK modulations with the number of rings as a constraint, we develop a generalized closed-form SER expression, and study the PAPR performance. In addition, we compare the scheme with M-QAM and M-PSK modulations, and provide experimental over-the-air results at 130 GHz. This modulation can be used as a building block of OFDM and DFT-S-OFDM systems to meet the Tbps goal.

The rest of the paper is organized as follows. In Sec. II, we provide details about the proposed modulation scheme, which includes constellation design, an estimate of SER with simulation results, and a comparison in terms of PAPR with the existing modulation schemes. In Sec. III, we describe the experimental setup, and present results comparing the different modulation techniques. The paper is concluded in Sec. IV.

II. M-ary Amplitude Phase Shift Keying

The proposed M-APSK modulation is adopted to enhance the THz band communication spectral efficiency by increasing the modulation order. The PAPR and SER performance of higher-order modulation are two crucial limiting factors to implement the schemes for THz ultrabroadband communication. By the proposed method, the PAPR is reduced compared to M-QAM by arranging the constellation points astutely over fewer constant amplitude rings. In addition, by arranging the constellation points into separate rings, the SER is improved significantly in contrast of the M-PSK

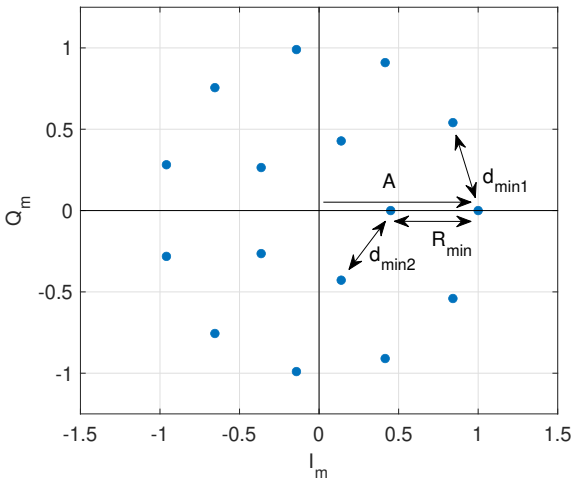

(a) Two-ring 16-APSK

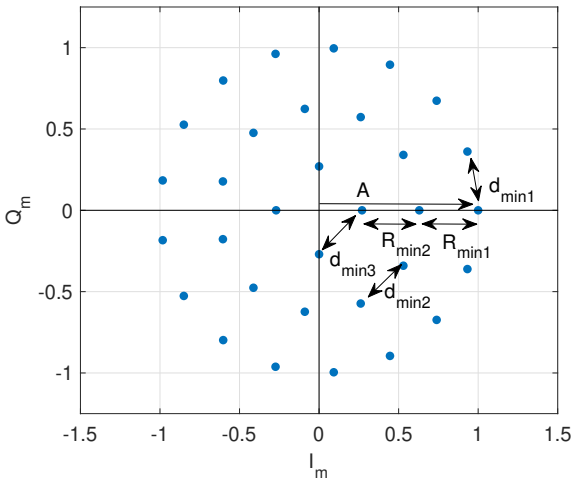

(b) Three-ring 32-APSK

Fig. 1: Constellation design with design criteria: a) 16-APSK with two rings; (b) 32-APSK with three rings to depict the different scenarios.

A. Constellation Design

The purpose of designing the constellation points is to optimize the minimum distance within the different concentric rings, i.e., keeping it same, while the M-ary points are divided into those separate amplitude rings similar to the PSK system. To satisfy the constant minimum distance between constellation points as well as between the rings (Fig. 1(a)), we keep the distance $d_{min1} = d_{min2} = R_{min}$ for the two-ring system. Therefore, the system design following the minimum distance equation of the M-PSK we have

$$\sin\left(\frac{\pi}{X}\right)2A = \sin\left(\frac{\pi}{M-X}\right)2A(A - \sin\left(\frac{\pi}{X}\right)2A), \quad (1)$$

where M is the modulation index, X and $M-X$ is the number of constellation points on the outer, i.e., a ring with maximum

amplitude, A, and inner ring, respectively. The separation between the rings is maintained by $A - \sin(\frac{\pi}{X})2A$.

Similarly, the constellation design equation for the 3 ring system (Fig. 1(b)) is based on $d_{min1} = d_{min2} = d_{min3} = R_{min1} = R_{min2}$ and given by

$$\begin{aligned}\sin\left(\frac{\pi}{X}\right)2A &= \sin\left(\frac{\pi}{Y}\right)2A(A - \sin\left(\frac{\pi}{X}\right)2A) \\ &= \sin\left(\frac{\pi}{M-X-Y}\right)2A(A - 2 \times \sin\left(\frac{\pi}{X}\right)2A),\end{aligned} \tag{2}$$

where Y is the number of constellation points in middle ring.

To find the solution for X, we use the approximation $\sin(\frac{\pi}{K}) \approx (\frac{\pi}{K})$, where K is the number of constellation points in any ring. The approximation satisfies closely if $K \geq 4$ (i.e., the approximation error < 0.1). In other words, the innermost ring should contain at least four constellation points. The solution for X with a two-ring system is obtained by solving (1), which can be written as

$$X = \left(\frac{M}{2}\right) + \pi, \tag{3}$$

and the solution for constellation points in innermost ring is $M - X$. In a similar fashion, (2) can be solved for the solution for X and Y for three-ring case which yields to

$$X = \left(\frac{M}{3}\right) + 2\pi, Y = X - 2\pi. \tag{4}$$

Here, the constellation points in the innermost ring is $M - X - Y$. Following these equation, the two-ring 16-APSK and 32-APSK corresponds to $X = 11$, $M - X = 5$ and $X = 19$, $M - X = 13$, respectively. Similarly, the three-ring 32-APSK yields to $X = 17$, $Y = 11$ with $M - X - Y = 4$ constellation points in the inner most ring. While the derived optimum constellation design is asymmetric, it can easily be changed to a symmetric one by rounding up the constellation points in each ring to the closest even number with slight increase in SER.

Further, the equations imposes limitations in the case of the minimum M requirement while utilizing specific number of rings, R. This constraint comes from i) comparing the maximum amplitude with the separation between the rings that need to be maintained, and ii) the number of constellation points in the innermost ring. Precisely, the constraint can be expressed as

$$A - \sin\left(\frac{\pi}{X}\right)2(R-1)A > 0, \tag{5}$$

and

$$C_{innermost} \geq 4, \tag{6}$$

respectively, where R is the number of rings we want to utilize and $C_{innermost}$ is the number of constellation points in the innermost ring. The system design should jointly obey both equations. Therefore, by substituting the value for X, Y and $C_{innermost}$ (i.e, M-X and M-X-Y for 2-ring and 3-ring, respectively) and solving them, we have the minimum number of M for a specific value for R. For example, the minimum number required for modulation index, M, is 16 and 32 for two and three-ring systems, respectively, considering that M is an integer of power of 2. Moreover, the solution can be extended for higher-order modulation, M, with added rings, R, in the same way. The scheme does not provide a proper fit for $M \leq 8$ schemes, making this complementary to the IEEE 802.15.3d standard schemes for low order modulation [9].

B. Symbol Error Rate

The theoretical SER for M-APSK can be obtained by solving the SER for the X-ary PSK, P_{XPSK} (largest ring), with a minimum distance of $d_{min} = \sin(\frac{\pi}{X})2A$, which is kept equal for any two adjacent points in any ring by design and the error introduced probabilistically due to the interaction of constellation points between the neighboring rings, P_{ring}. Therefore, the SER depends on the number of rings utilized for the system and decreases as the number of ring increases, which is directly related to the decrease in the number of X. The expression for P_{XPSK} (i.e., intra-ring error probability) is given by

$$P_{XPSK} = 2Q\left(\frac{\sin(\pi/X)2A}{\sqrt{2N_0}}\right), \tag{7}$$

where N_0 is noise power spectral density. Furthermore, there are contributing terms in the effective/total SER due to the error incorporated by one ring's constellation points to the other rings. It can be statistically shown that the inter-ring error probability decreases with the decrease in constellation points of the inner rings compare to the outermost ring's constellation point, X. So, the expression for the two-ring system is given by

$$\begin{aligned}P_{2ring} \approx \frac{1}{2 \times 2}\Bigg[2\frac{M-X}{X}Q\left(\frac{\sin(\pi/X)2A}{\sqrt{2N_0}}\right) \\ + 2\frac{M-X}{X}Q\left(\frac{2(A - \sin(\pi/X)2A)}{\sqrt{2N_0}}\right)\Bigg].\end{aligned} \tag{8}$$

Similarly, for three-ring system, the SER due to interaction between the rings is given by

$$\begin{aligned}P_{3ring} \approx \frac{1}{2 \times 3}\Bigg[2\frac{Y}{X}Q\left(\frac{\sin(\pi/X)2A}{\sqrt{2N_0}}\right) \\ + 2\frac{M-X-Y}{X}Q\left(\frac{\sin(\pi/X)2A}{\sqrt{2N_0}}\right) \\ + 2\frac{M-X-Y}{X}Q\left(\frac{2(A - \sin(\pi/X)4A)}{\sqrt{2N_0}}\right)\Bigg].\end{aligned} \tag{9}$$

The above equation can be extended for higher-order modulation with more number of rings in same way. Therefore, the effective/total SER for M-APSK, P_{eff}, is obtained by

$$P_{eff} = 1 - (1 - P_{XPSK})(1 - P_{ring}), \tag{10}$$

which can be approximated as

$$P_{eff} = P_{XPSK} + P_{ring}. \tag{11}$$

The comparison of SER of M-QAM, M-PSK, and M-APSK is shown in Fig. 2 for $M = 16$ and $M = 32$. It is observable that the simulated SER closely matches with the analytical result, which confirms our numerical calculation. The slight mismatch is due to the approximation of constellation points

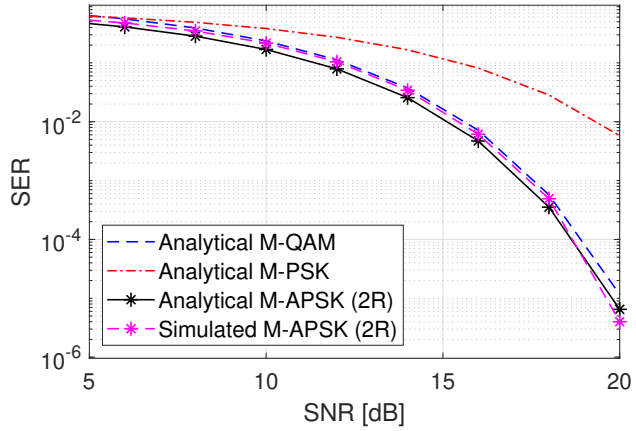

(a) M=16

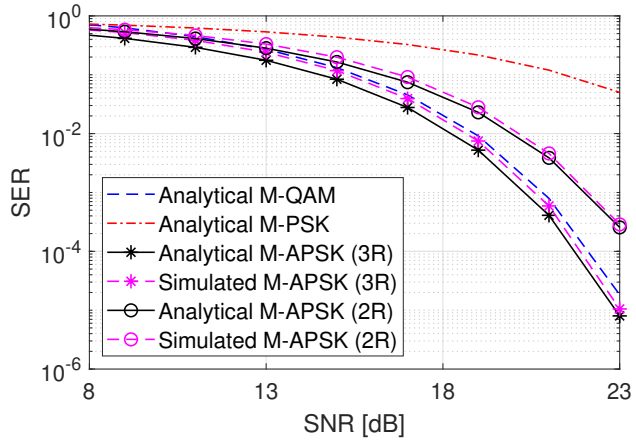

(b) M=32

Fig. 2: SER comparison between M-QAM, M-PSK, and M-APSK with increasing SNR: a) M=16; (b) M=32.

in a particular ring to the nearest integer value. It is depicted that the performance of M-APSK is better than M-PSK in both cases. However, there is a small improvement compared to M-QAM if the maximum number of rings is utilized for M-APSK, i.e., $R = 2$ for $M = 16$ and $R = 3$ for $M = 32$. M-QAM functions better than M-APSK if the ring number is reduced. This is a trade-off with PAPR.

C. Peak to Average Power Ratio

The PAPR is one of the essential metrics that restricts the utilization of spectral efficient modulation techniques, such as conventional high-order QAM, OFDM for THz band communication, which arises mainly due to the front-end electronics' efficiencies at THz frequencies dominated by the PAs. Literature shows that the P_{sat}, gain and efficiency decrease by following $\frac{1}{f_c^2}$ relation [18]. Therefore, in most cases, the single-carrier communication waveform with a low modulation index is proposed for THz band communication. The M-APSK scheme has a comparatively low- PAPR than other amplitude modulation schemes. The constellation points are suitably divided into fewer constant amplitude rings to reduce the PAPR as well as SER. However, the PAPR is increased with the number of rings utilized to split the points. The average power, P_{avg}, of the scheme with two/three-rings is given by,

$$P_{avg-2R} = \frac{1}{M}[XA^2 + (M-X)(A - \frac{\pi}{X}2A)^2], \quad (12)$$

$$P_{avg-3R} = \frac{1}{M}[XA^2 + Y(A - \frac{\pi}{X}2A)^2 + (M-X-Y)(A - \frac{\pi}{X}4A)^2], \quad (13)$$

respectively, where, A^2 is the peak power.

TABLE I: Comparison of PAPR.

Modulation	PAPR (dB)	
	M=16	M=32
PSK	0	0
QAM	2.5	3.2
M-APSK 2R/3R	1.22/NA	1.08/1.73

In Table I, the comparison of PAPR between M-APSK, M-PSK and M-QAM is shown. It is observable that the PAPR is reduced considerably compared to the M-QAM counterpart.Also, the PAPR decreases with the number of rings. However, the PAPR for the M-PSK scheme is the lowest among the three and is 0 dB. Therefore, the system design supports utilizing the higher-order schemes while keeping the PAPR in considerable range and could be utilized to increase the spectral efficiency without the performance degradation due to PA limitations. Besides, as the number of rings provides a trade-off between PAPR and SER, it can be utilized as a design metric depending on the system requirement.

III. Experimental Setup and Results

In this section, experimental results are provided by comparing M-APSK, M-PSK, and M-QAM modulations. The offline 32-GHz signal processing back-end with 120-140 GHz front-ends presented in [19] are utilized for the purpose.

A. Experimental Setup

The 120-140 GHz front-ends (Fig. 3 (top)) are custom-designed by Virginia Diodes Inc. (VDI) and consist of two frequency doublers to generate the required carrier signal at the transceiver. At the transmitter, a mixer with 7 dB of double sideband conversion loss and 20 GHz of bandwidth is utilized to modulate the carrier signal with the information-bearing baseband (BB)/intermediate frequency (IF) signal. The system provides a maximum output power of 13 dBm at radio frequency (RF). At the receiver, a low noise mixer is utilized to obtain the IF signal from RF. Furthermore, 38 dBi antennas are utilized on both transceiver sides for closing the link budget.

To generate the BB/IF, an offline digital back-end system based on an arbitrary waveform generator (AWG) at the transmitter and a digital storage oscilloscope (DSO) at the receiver is utilized. A software-defined physical layer is used to define and generate the BB/IF signals at the transmitter and, correspondingly, collect and process them at the receiver [20].

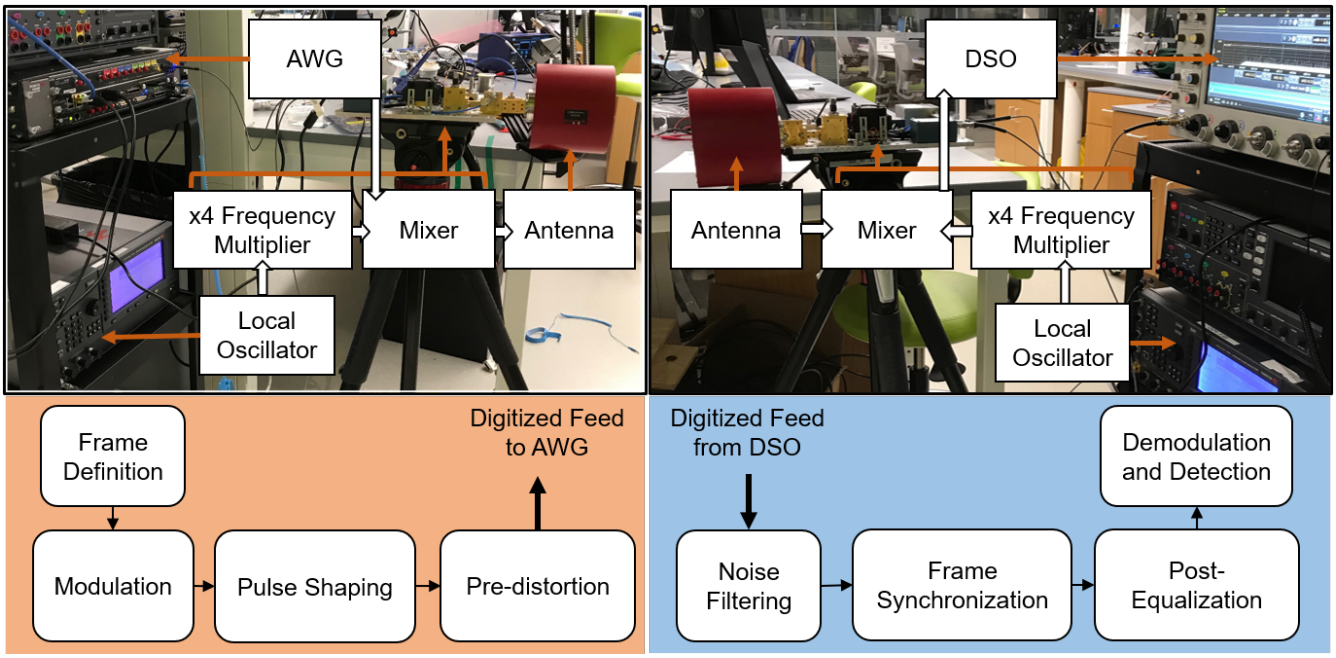

Fig. 3: The 120-140 GHz testbed and schematic diagram of hardware components (top); and diagram of the software-defined physical layer (bottom) for transceiver system.

MATLAB is chosen as the environment to develop the different signal processing blocks (Fig. 3 (bottom)), such as frame definition, modulation, pulse shaping, and pre-distortion filter at the transmitter with noise filtering, frame synchronization, post-equalization, and demodulation at the receiver.

B. Experimental Results

To compare the experimental bit error rate (BER) performance of the M-APSK, M-PSK, and M-QAM schemes at THz frequencies, the modulated IF signals are up-converted to 130 GHz. It is noted here that, for the experimental results, BER is considered instead of SER to show the performance at bit-level. Furthermore, in the case of M-PSK and M-QAM, the grey coding is used, whereas, for M-APSK, binary coding is implemented since the grey code conversion is challenging [21]. In this case, IF modulated signals of up to 20 GHz bandwidth with data-rate up to 50 Gbps are considered varying distances until 15 m. In Table II and III, we summarize the results of different schemes. To calculate the BER, ten-frames are considered (each 1,200 bits long).

It is observable from the experimental result that the BER of 16-PSK and 32-PSK comparatively higher than the corresponding M-QAM and M-APSK counterparts. Although the PAPR is low, the M-PSK is not a suitable candidate for the high-order modulation schemes when utilized for ultrabroadband communication for THz frequencies. It is noticeable that the BER of two-ring 16-APSK and three-ring 32-APSK are better than 16-QAM and 32-QAM, respectively. Furthermore, two-ring 32-APSK performance is quite close to the 32-QAM system. The reseason behind the reduced performance of the M-QAM is the higher PAPR compare to the M-APSK scheme. It is depicted in the corresponding captured SNR for the schemes mentioned above, where PSK has a maximum captured SNR followed by M-APSK and QAM. Due to the damage limit constraint of the front-end's input power, we have maintained the peak power for all the schemes same. Moreover, the transceiver chains have a PA to boost the received signal's power, which imposes restrictions towards the utilization of signals with high PAPR. Added, the non-linearity and frequency selective response due to the ulrabroadband devices, the performance of all the schemes are relatively impoverished compared to the normal AWGN channel and relatively prominent in the case of 10 GHz baseband siganls than the 5 GHz one. Thus, the experimental results motivate us to utilize the M-APSK for ultrabrodband THz band communication when utilizing the constellation scheme with high modulation index, M.

IV. Conclusion

The THz band is gaining much attention as it offers the bandwidth needed to cope with the ever-increasing data rate demands expected in next-generation wireless systems. Despite the major progress in THz device technologies, there are several limitations associated with the efficiency and response of THz devices that require non-traditional signal processing techniques. The paper proposes a modified M-ary APSK to achieve high spectral efficiency in ultrabroadband communications. While the performance of 16 and 32-APSK with two and three rings are shown, the expression related to constellation design, closed-form SER, and PAPR can easily be extended for higher-order modulation with varying numbers of rings. The proposed technique is designed to achieve better SER than PSK systems and comparable/better BER performance

TABLE II: BER comparison for different modulation schemes with 5 GHz baseband bandwidth.

Distance (m)		3		9		15	
Modulation	Data Rate (Gbps)	SNR (dB)	BER	SNR (dB)	BER	SNR (dB)	BER
16-PSK	20	29	0*	20.9	0*	16.5	8×10^{-5}
16-QAM	20	27.5	0*	18	0*	13.1	0*
16-APSK 2R	20	28.7	0*	19.1	0*	13.5	0*
32-PSK	25	29.6	1.6×10^{-3}	21	5×10^{-3}	15.8	8×10^{-3}
32-QAM	25	28.1	0*	18.2	2.5×10^{-4}	13.2	5×10^{-4}
32-APSK 2R	25	27.7	0*	19.5	1.6×10^{-4}	14	5.8×10^{-4}
32-APSK 3R	25	27.7	0*	19.5	0*	14	8×10^{-5}

*0 BER: no bit error within 10 frames with 1,200 bits each.

TABLE III: BER comparison for different modulation schemes with 10 GHz baseband bandwidth.

Distance (m)		3		9		15	
Modulation	Data Rate (Gbps)	SNR (dB)	BER	SNR (dB)	BER	SNR (dB)	BER
16-PSK	40	26.2	1.9×10^{-2}	17.3	3.7×10^{-2}	13.9	4.4×10^{-2}
16-QAM	40	24	4.1×10^{-3}	15.1	2×10^{-2}	11.2	3.2×10^{-2}
16-APSK 2R	40	25	0*	16.5	4.1×10^{-3}	12	1.5×10^{-2}
32-PSK	50	25.9	7×10^{-2}	17.5	1.5×10^{-1}	13.2	1.8×10^{-1}
32-QAM	50	23.1	1.8×10^{-2}	15.5	7×10^{-2}	11.1	8×10^{-2}
32-APSK 2R	50	25.1	1.5×10^{-2}	17.5	1.1×10^{-1}	12	1.3×10^{-1}
32-APSK 3R	50	24.9	2.5×10^{-3}	17.1	9×10^{-2}	11.5	1×10^{-2}

*0 BER: no bit error within 10 frames with 1,200 bits each.

compared to QAM systems while alleviating the high PAPR problem in QAM modulations. The proposed techniques have been experimentally validated at 120–140 GHz band achieving bit-rates of the order of 50 Gbps. Future extending the work is aimed at in-depth fixed-point analysis of the proposed scheme, thereby investigating the actual digital hardware complexity/cost associated with the proposed technique. In addition, the scheme performance in the presence of phase noise compared to the traditional schemes will be studied, all prior to testing the performance of a M-APSK-OFDM setup.

REFERENCES

[1] K. Sengupta, T. Nagatsuma, and D. M. Mittleman, "Terahertz Integrated Electronic and Hybrid Electronic–Photonic Systems," *Nature Electronics*, vol. 1, no. 12, pp. 622–635, 2018.

[2] Z. Chen, X. Ma, B. Zhang, Y. Zhang, Z. Niu, N. Kuang, W. Chen, L. Li, and S. Li, "A survey on terahertz communications," *China Communications*, vol. 16, no. 2, pp. 1–35, 2019.

[3] S. Nie, J. M. Jornet, and I. F. Akyildiz, "Intelligent environments based on ultra-massive mimo platforms for wireless communication in millimeter wave and terahertz bands," in *ICASSP 2019 - 2019 IEEE International Conference on Acoustics, Speech and Signal Processing (ICASSP)*, 2019, pp. 7849–7853.

[4] T. S. Rappaport, Y. Xing, O. Kanhere, S. Ju, A. Madanayake, S. Mandal, A. Alkhateeb, and G. C. Trichopoulos, "Wireless communications and applications above 100 ghz: Opportunities and challenges for 6g and beyond," *IEEE Access*, vol. 7, pp. 78 729–78 757, 2019.

[5] H. Han *et al.*, "Design of thz space application system," *Journal of Computer and Communications*, vol. 3, no. 03, p. 61, 2015.

[6] J. M. Jornet and I. F. Akyildiz, "Channel Modeling and Capacity Analysis for Electromagnetic Wireless Nanonetworks in the Terahertz Band," *IEEE Transactions on Wireless Communications*, vol. 10, no. 10, pp. 3211–3221, 2011.

[7] D. Wang, M. Zhang, Z. Cai, Y. Cui, Z. Li, H. Han, M. Fu, and B. Luo, "Combatting Nonlinear Phase Noise in Coherent Optical Systems with an Optimized Decision Processor based on Machine Learning," *Optics Communications*, vol. 369, pp. 199–208, 2016.

[8] H. Sarieddeen, M.-S. Alouini, and T. Y. Al-Naffouri, "An overview of signal processing techniques for terahertz communications," *arXiv preprint arXiv:2005.13176*, 2020.

[9] "Ieee standard for high data rate wireless multi-media networks–amendment 2: 100 gb/s wireless switched point-to-point physical layer," *IEEE Std 802.15.3d-2017 (Amendment to IEEE Std 802.15.3-2016 as amended by IEEE Std 802.15.3e-2017)*, pp. 1–55, 2017.

[10] Z. Yu, R. J. Baxley, and G. T. Zhou, "Iterative clipping for papr reduction in visible light ofdm communications," in *2014 IEEE Military Communications Conference*, 2014, pp. 1681–1686.

[11] J. Hancock and R. Lucky, "Performance of combined amplitude and phase-modulated communication systems," *IRE Transactions on Communications Systems*, vol. 8, no. 4, pp. 232–237, 1960.

[12] W. Weber, "Differential encoding for multiple amplitude and phase shift keying systems," *IEEE Transactions on Communications*, vol. 26, no. 3, pp. 385–391, 1978.

[13] H. Rohling and V. Engels, "Differential amplitude phase shift keying (dapsk)-a new modulation method for dtvb," 1995.

[14] X. Xiang and M. C. Valenti, "Closing the gap to the capacity of apsk: Constellation shaping and degree distributions," in *2013 International Conference on Computing, Networking and Communications (ICNC)*. IEEE, 2013, pp. 691–695.

[15] D. ETSI, "Document etsi en 302 307 v1. 2.1 (2009-08)," *Digital Video Broadcasting (DVB)*.

[16] W. Sung, S. Kang, P. Kim, D.-I. Chang, and D.-J. Shin, "Performance analysis of apsk modulation for dvb-s2 transmission over nonlinear channels," *International Journal of Satellite Communications and Networking*, vol. 27, no. 6, pp. 295–311, 2009.

[17] A. R. Ndjiongue, H. C. Ferreira, and T. M. Ngatched, "Closed-form ser expression for apsk based on the kite structure," *IEEE Communications Letters*, vol. 21, no. 10, pp. 2182–2185, 2017.

[18] H. Wang, F. Wang, H. Nguyen, S. Li, T. Huang, A. Ahmed, M. Smith, N. Mannem, and J. Lee, "Power amplifiers performance survey 2000-present," *Georgia Tech Electronics and Micro-System Lab (GEMS)*, 2018.

[19] P. Sen, V. Ariyarathna, A. Madanayake, and J. M. Jornet, "Experimental wireless testbed for ultrabroadband terahertz networks," in *Proceedings of the 14th International Workshop on Wireless Network Testbeds, Experimental evaluation & Characterization*, 2020, pp. 48–55.

[20] P. Sen, D. A. Pados, S. N. Batalama, E. Einarsson, J. P. Bird, and J. M. Jornet, "The teranova platform: An integrated testbed for ultra-broadband wireless communications at true terahertz frequencies," *Computer Networks*, vol. 179, p. 107370, 2020.

[21] Z. Liu, Q. Xie, K. Peng, and Z. Yang, "Apsk constellation with gray mapping," *IEEE Communications Letters*, vol. 15, no. 12, pp. 1271–1273, 2011.